J. Phys. B: At. Mol. Opt. Phys. 27 (1994) 4195–4213. Printed in the UK

Excitation of atomic hydrogen by protons and multiply charged ions at intermediate velocities

D Detleffsen, M Anton, A Werner and K-H Schartner

I Physikalisches Institut, Justus-Liebig-Universität Giessen, Heinrich-Buff-Ring 16, 35392 Giessen, Germany

Received 16 May 1994, in final form 29 June 1994

Abstract. We have investigated the collisional excitation of hydrogen atoms by protons and multiply charged ions at intermediate velocities applying the optical method. The population of the np levels ($n=2,\ldots,6$) has been determined for a variety of projectiles with charge states q ranging from 1+ to 11+ and scaled velocities $v/\sqrt{q}$ between 0.7 and 5.6 au. The cross sections are shown to fulfil the scaling relation $\sigma/q=f(v^2/q)$ with respect to the projectile charge q and velocity v for $q\geqslant 3$. The relevance of scaled intermediate velocities for a classification of excitation mechanism is pointed out.

1. Introduction

The hydrogen atom or, more generally, the ionic one-electron system is of fundamental interest for testing the theoretical description of atomic structures. In a corresponding way the hydrogen atom serves as a fundamental target in atomic collision studies. Its wavefunctions are well known and therefore the different methods applied in theoretical atomic collision studies are tested by themselves. As a consequence a large variety of methods treating excitation in atomic collisions have been applied to the $H^+ + H$ system. The earlier results are summarized in, e.g., Massey and Gilbody (1974) while for the recent work Fritsch and Lin (1991) may be used for references. In contrast, only a small number of experiments have been reported which study the excitation of atomic hydrogen by protons. Excitation by highly charged ions is reported in the following for the first time. The small number of experiments is due to the experimental difficulties of providing a well defined target of dissociated hydrogen in combination with an efficient dispersion and detection system for the ion impact induced fluorescence radiation and with the often limited flux of highly charged ions.

Fritsch and Lin (1991) refer especially to the range of intermediate impact velocities which is, at least for proton impact, the range of the presented study. In this range, generally defined by the projectile velocity and the orbit velocity of the active target electron being comparable, capture processes, excitation and ionization channels are of the same order of magnitude and moreover influence each other strongly. In the low velocity range often only few or even two interacting molecular states can reveal the main physical collision mechanism whereas in the range of large impact velocities perturbative two-state models are successful. In contrast a large number of states of atomic or molecular character have to be considered at intermediate velocities. Though the

0953-4075/94/184195+19$19.50

number of these states can become rather large and a simple interpretation of the excitation mechanism is then impossible, a restriction to a few states allowing a closed form solution of the problem sometimes leads to a more global understanding of the elementary features of the studied process. This is the case in the systematic investigation of excitation of the np states in hydrogen by structureless ions of charge q by Janev and Presnyakov (1980). Limiting the basis set to three atomic states and applying a dipole approximation to the interaction potential, Janev and Presnyakov (1980) derived a scaling relation (in the following text referred to as JP scaling) for the excitation cross section σ as a function of the scaled impact velocity v,

$$\sigma/q = f(v^2/q).$$

The physical relevance of the scaling of the projectile velocity is that $v/\sqrt{q}$ has to be used in characterizing the range of intermediate velocities (Reinhold *et al* 1990). The approximations applied by Janev and Presnyakov (1980) were tested by Fritsch and Schartner (1987) and by Fritsch *et al* (1991) with results discussed in the following. The aim of the presented experiments is a study of to what extent the JP scaling holds for the processes

$$A^{q+} + H \rightarrow A^{q+} + H^*(np) \qquad n = 2, \ldots, 6, q = 1, \ldots, 11.$$

In former studies of our group of the excitation of He by highly charged ions (Reymann *et al* 1988, Anton *et al* 1992, 1993) the validity of the JP scaling was shown for $q > 2$. The results indicated that the universal function f is slightly different for protons and for highly charged ions.

Additional to the fundamental interest, the presented study is motivated by the importance of the measured cross sections for modelling the stopping power of neutral hydrogen atoms which are used for plasma heating by neutral beam injection (Janev *et al* 1989).

2. Experiment

The experiments were performed at the 1 MV van de Graaff accelerator in Giessen and at the 4 MV tandem and the 400 kV electrostatic accelerators of the Dynamitron-Tandem Laboratory in Bochum. Protons with energies between 40 keV and 800 keV, He^{2+} ions with scaled energies E/mq between 40 keV u^{-1} and 120 keV u^{-1}, Si^{q+} ions ($q = 2, \ldots, 9$) with scaled energies between 23.8 keV u^{-1} and 190.5 keV u^{-1}, and Cu^{q+} ions ($q = 3, \ldots, 11$) with scaled energies between 12.7 keV u^{-1} and 63.6 keV u^{-1} were used. A schematic view of the experimental set-up is shown in figure 1. The ion beam was collimated and collected in a Faraday cup. An electron beam from a television type gun could replace the ion beam. A beam of ~90% dissociated hydrogen from a RF source was crossed with the ion beam. The residual pressure in the intersection region with the RF source on was about 2×10^{-5} Torr.

A 1 m normal incidence monochromator (McPherson 225) was mounted under the double magic angle in order to avoid corrections for the unknown polarization of the observed light (Clout and Heddle 1969). The monochromator was equipped with a position-sensitive channelplate detector of the wedge and strip type. It was possible to record the complete Lyman series of the hydrogen atom in a single measurement. The spectral resolution was sufficient to separate for the $H^+ + H$ system the Doppler-shifted projectile lines from the target lines. A recombination trap for atomic hydrogen was

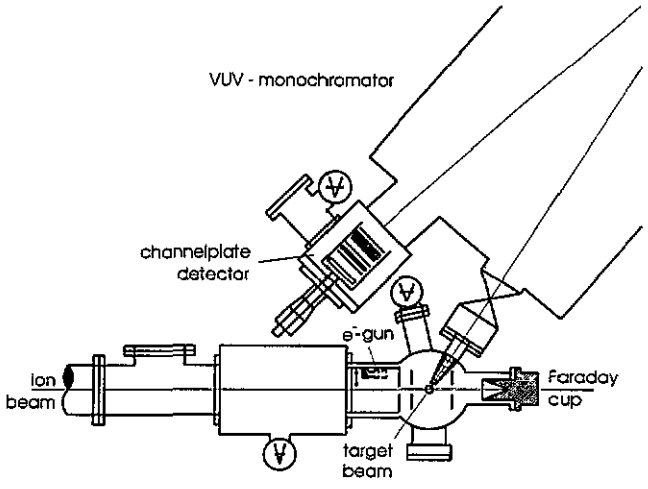

Figure 1. Experimental set-up.

mounted in the optical path between target beam and monochromator to suppress the resonance absorption of the Lyman lines by the hydrogen atoms in the residual gas. The trap consists of a tube made from a stainless steel net. To enlarge the surface some diaphragms were fixed inside the tube. Because hydrogen atoms recombine effectively on metal surfaces, the partial pressure of the atoms in the trap is significantly reduced. The recombination trap helped to increase the transmission of the Lyman-α line by more than a factor 3 to about 80%.

The RF discharge source was operated at 30 MHz with a power of 30 W. The dissociated hydrogen was transported through a 10 cm long Pyrex tube terminated by a short 2 mm × 1 mm PTFE canal just above the intersection region. The slit of the nozzle was oriented parallel to the ion beam in order to increase the observed target length. The gas flow through the source was controlled by a mass flow controller and was kept constant within 1%. The target density, averaged over the observation length of 1 cm of the detection system, was some 10^{11} cm^{-3}.

The degree of dissociation D was determined *in situ* by recording the signal of Werner bands of H_2 after electron excitation with the discharge switched either on and off, respectively. Because the mass flow through the source was constant, D is given by:

$$D = 1 - S_{on}(H_2)/S_{off}(H_2) \quad (1)$$

where $S(H_2)$ is the signal of the Werner band. In the spectral region used, between 104 and 120 nm, there are no resonance lines of H_2, so there is no problem with resonance absorption of molecular lines. Because the molecular signal with the discharge on is of the same magnitude as the detector background, one has to subtract the background. To correct a spectrum recorded with the discharge on for the molecular signal from the hydrogen being not dissociated and from the molecules in the background gas, a second spectrum with the discharge off was always recorded. This molecular spectrum was multiplied by a factor $(1 - D)$ and subtracted from the spectrum with the discharge on. Figures 2 and 3 show spectra from 3 keV electron impact excitation of the effusive beam with RF discharge on or off, respectively.

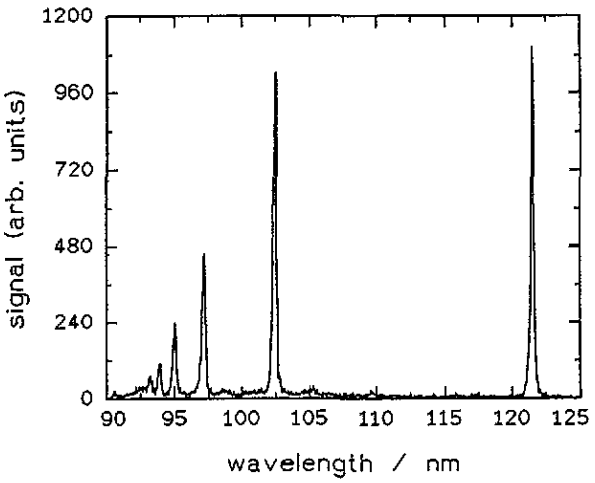

Figure 2. Spectrum of atomic hydrogen from 3 keV electron impact excitation.

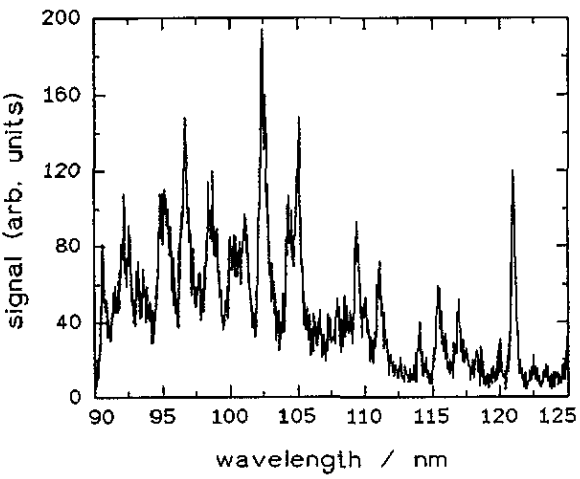

Figure 3. Spectrum of molecular hydrogen from 3 keV electron impact excitation.

The population of a collisionally excited atomic level $|i\rangle$ is measured by the intensity of the fluorescence light, which is emitted in a transition from the excited state to a lower lying level $|j\rangle$. The signal state S_{ij} per incident projectile at fixed target density is a measure of the excitation cross section. Absolute cross sections were obtained by normalization on experimentally or theoretically determined excitation cross sections σ_i^n

$$\sigma_i^{q+} = \sigma_i^n \frac{S_{ij}^{q+}}{S_{ij}^n}. \tag{2}$$

The index n denotes the known process, $q+$ the process for which the cross section is of interest. The cascade contribution was not explicitly taken into account, but is implicitly included by the normalization on excitation cross sections σ_i^n. Model calculations based on the FBA allowed the estimate that the cascade signal contributes less than 5% to the cross sections.

3. Results and discussion

All cross sections and their error bars are tabulated. The latter have the same value for the excitation of each *n*p state by the same projectile. They contain the statistical uncertainty and the uncertainty of the cross section used for normalization.

3.1. H^+–H collisions

The cross sections for collisional excitation of H(2p) by protons are presented in figure 4. They are normalized for each level on the first Born approximation (FBA) (Mandal *et al* 1990) at 400, 500, 600 and 800 keV by taking the average of σ_i^n/S_{ji}^n at these energies. For comparison the experimental results of Stebbings *et al* (1965), Morgan *et al* (1973) and Kondow *et al* (1974) and some selected calculations are included. The

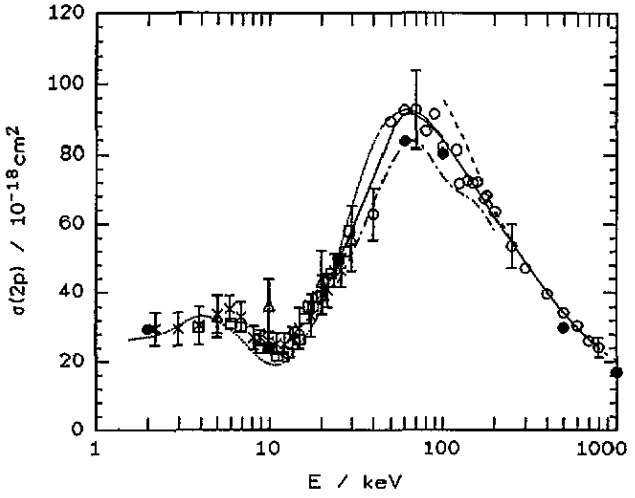

Figure 4. Cross sections for the excitation of the 2p state by protons. Experiment: ○, present data; ——, averaged curve; △, Stebbings *et al* (1965); ×, Morgan *et al* (1973); □, Kondow *et al* (1974). Theory: · · · ·, CC, Fritsch and Lin (1983); – – –, FBA, Mandal *et al* (1990); — · —, EIA⁻, Rodriguez and Miraglia (1992); ●, doorway approximation, Henne *et al* (1993).

experimental data cover the energy range from ~1 to 800 keV. Our own data show a good agreement with the cross sections measured by the other groups. To compare the cross sections for the $H^+ + H$ collisions with the cross sections measured after excitation by the heavier projectiles, an averaged curve is derived from the data of Kondow *et al* and our own data for energies greater than 20 keV.

Only the more recent calculations were inserted in figure 4. The earliest of the here selected theories are the close coupling calculations of Fritsch and Lin (1983). These authors used a two-centre expansion with a supplement of united atom orbitals (AO+) to describe molecular effects at low energies. The ionization channel is accounted for by the use of 'pseudostates'. The calculations show a very good agreement with the experiments. Both the minimum of the cross sections at 12 keV and the maximum between 60 keV and 70 keV are precisely described with respect to position and magnitude. Henne *et al* (1993) carried out close coupling calculations with only 10 target-centred states. The states which were not explicitly considered in their base were included

by means of an optical potential in the 'doorway' approximation. The results also show a very good agreement with the experimental data with the remarkable fact that the calculations cover the complete energy range of the experiments. From 200 keV on the FBA (Mandal *et al* 1990) is sufficient to describe the data. Exemplary for distorted wave calculations, the symmetric eikonal approximation of Rodriguez and Miraglia (1992) demonstrates a quite good description of the excitation process for energies greater than 25 keV.

The only available experimental data for higher n values are measurements by Park *et al* (1976), who investigated the excitation of the H($n=3$) level and measurements of the Balmer-α emission cross sections by Donnelly *et al* (1991). The latter data deviate remarkably from the calculations by Shakeshaft (1978) and motivated further recent calculations by Ermolaev (1991) and by Slim (1993). The Balmer-α emission cross section can be expressed by the excitation cross sections of the l-states of the $n=3$ level in the following way:

$$\sigma(H_\alpha)=\sigma(3s)+0.12\sigma(3p)+\sigma(3d)=\sigma(n=3)-0.88\sigma(3p) \tag{3}$$

where the factor 0.12 results from the branching ratio of the H(3p) to the H(2s) transition. From equation (3) it is possible to calculate a Balmer-α emission cross section from the data of Park *et al* (1976) and from our own 3p cross sections. The data of Park *et al* (1976) were renormalized to the FBA at 200 keV as suggested by various authors (e.g. Ermolaev (1991)). The Balmer-α emission cross sections of Donnelly *et al* and our indirectly measured cross sections are presented in figure 5. Though the error bars are quite large (two cross sections of comparable magnitude have to be subtracted according to equation (3)) it is obvious that the two data sets do not agree. Our cross sections confirm the close coupling calculations mentioned above. To clarify the discrepancy, the Balmer-α emission cross section should be reinvestigated.

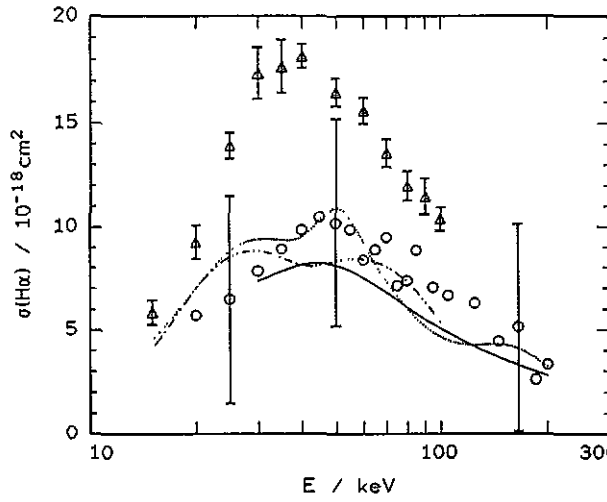

Figure 5. Cross section for Balmer-α emission after excitation by protons. Experiment: O, present data calculated with equation (3) from the data of Park *et al* (1976) and our own data; △, Donnelly *et al* (1991). Theory: ——, CC, Ermolaev (1991); · · · ·, CC, Shakeshaft (1978); — · · —, CC, Slim (1993).

3.2. He^{2+}–H collisions

The success of the close coupling method at intermediate velocities, demonstrated for the H^+–H system in the preceding section, is encouraging for an application to the He^{2+}–H system. Due to the stronger binding of the electron in He^+, more and especially higher projectile states have to be taken into account in comparison with the H^+–H system. Moreover, the cross sections for excitation of the *n*p states allow a first test of the validity of the JP scaling. Consequently the following data for He^{2+} impact are plotted in the scaled relation σ/q against E/mq.

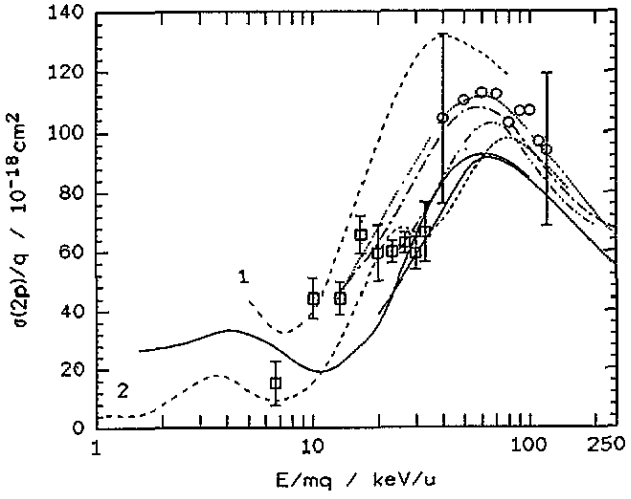

Figure 6. Cross sections for the excitation of the 2p state by He^{2+} ions. Experiment: ○, present data; □, Hughes *et al* (1993); · · · ·, averaged He^{2+} data; ——, averaged proton data and CC calculations of Fritsch *et al* (1991) for excitation by protons. Theory: 1 – – –, CC, Fritsch and Schartner (1987); 2 – – –, CC, Fritsch *et al* (1991); — · —, CC, Bransden *et al* (1983); — · · —, EIA⁻, Rodriguez and Miraglia (1992).

Figure 6 shows our data in comparison with the only other published data of Hughes *et al* (1993). The two displayed data sets differ by about 40% at 40 keV u^{-1} where the energy ranges of both experiments join. Below this energy the data of Hughes show a plateau and decrease for energies smaller than 15 keV u^{-1}. Combining both data sets, a clear structure is observable. Unpublished data in the 5 keV scaled energy range, cited by Fritsch *et al* (1991), were not inserted in figure 6. They agree satisfactorily with the calculations by Fritsch *et al* (1991).

Turning now to the comparison of experiment and calculation, close coupling calculations by Bransden *et al* (1983) were performed with a target-centred base of 19 Slater-type states and pseudostates. Below 37.5 keV u^{-1} the base is supplemented by projectile-centred 1s, 2s and 2p states to consider electron capture. The calculations agree well with the data, but the structure observed by Hughes *et al* (1993) is not predicted. AO+ close coupling calculations of Fritsch and Schartner (1987) overestimate the data by about 10% and also do not show any structure between 15 keV u^{-1} and 40 keV u^{-1}. Later Fritsch *et al* (1991) extended the AO+ basis used. The new calculations describe the data well at low and high energies, but now show a structure between 25 keV u^{-1} and 80 keV u^{-1} which was confirmed by Hughes *et al* (1993). More pronounced is a structure in the calculations of the cross section for the 3p excitation, as shown in

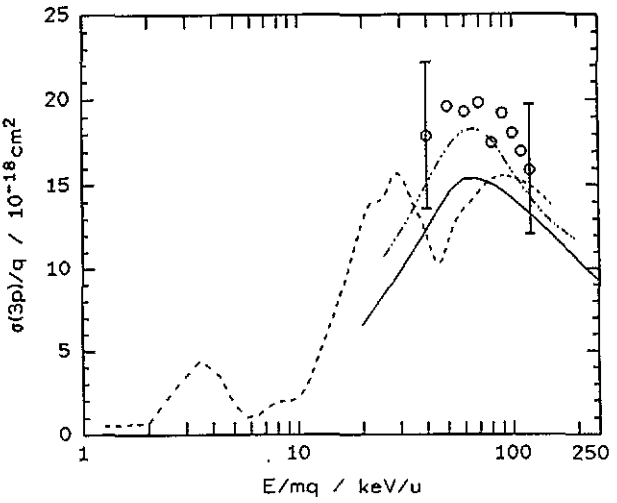

Figure 7. Cross sections for the excitation of the 3p state by He^{2+} ions. Experiment: O, present data; ——, averaged proton data. Theory: - - -, CC, Fritsch *et al* (1991); — · · —, EIA⁻, Rodriguez and Miraglia (1992).

figure 7. It is shifted towards higher energies, thus allowing a direct comparison with our data which to the contrary behave smoothly. For the 3p excitation by He^{2+} ions no further data are available for comparison. Furthermore, figures 6 and 7 include symmetric eikonal calculations by Rodriguez and Miraglia (1992). The agreement with the experimental data is rather good, but also in this case no structure is predicted. In conclusion, there remains the question, whether the discussed structures are an artifact depending on the choice of the basis states. This problem is momentarily investigated for the H^+–H system in studies of the calculated energy dependence of the 2p level excitation cross section, varying the number of projectile- and target-centred basis states, by Slim (1994).

For the following comparison with other projectiles an averaged curve is drawn through the data points for He^{2+} impact, subjectively ignoring any structures. This averaged scaled curve lies about 20% above the mean curve through the proton data and the position of the cross section maximum is slightly shifted towards lower energies.

3.3. A^{q+}–H collisions

Figure 8 shows the scaled cross sections for excitation of the H(2p) level by $Si^{2,3,4,5,6,7,8,9+}$ and $Cu^{5,6+}$ ions as a function of the scaled energy. The cross sections are normalized on cross sections for excitation by 150 and 200 keV protons and alternatively by 3 keV electrons. The large error bars, compared with the errors of the cross sections measured with the other projectiles, are the result of various technical problems during the measurements. For comparison the averaged curves through the H^+ and the He^{2+} data are included.

The scaled cross sections for all Si and Cu projectiles lie within the error bars on a universal curve. The energy dependence is very similar to the case of proton and He^{2+} excitation, in particular the excitation function does not exhibit any structure between 15 keV u^{-1} and 40 keV u^{-1}. Figure 8 suggests that for $q \geqslant 3$ an universal relation $\sigma/q = f(v^2/q)$ exists, but that the proton and He^{2+} impact data deviate (slightly) from this

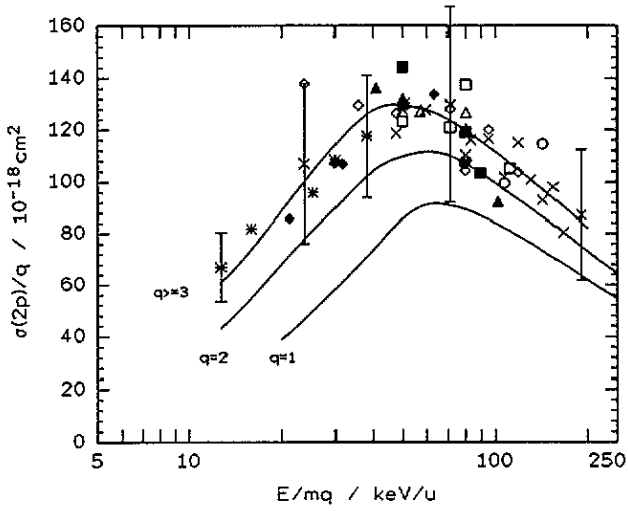

Figure 8. Scaled cross sections for the excitation of the 2p state by Cu and Si ions. Experiment: ○, Si^{2+}; ×, Si^{3+}; □, Si^{4+}; △, Si^{5+}; ◇, Si^{6+}; ▲, Si^{7+}; ■, Si^{8+}; ●, Si^{9+}; ✱, Cu^{5+}; ◆, Cu^{6+}; ——, averaged data for excitation by protons, He^{2+}, Si^{q+} and Cu^{q+}.

universal function: i.e. the JP scaling holds for $q \geqslant 3$. Furthermore the maximum of the scaled cross sections is shifted towards smaller energies with increasing projectile charge q. This behaviour is analogous to the excitation of the 3^1P state of helium (Anton *et al* 1993). However in this case the difference of the scaled curves for $q=2$ and $q \geqslant 3$ is not so clear.

A comparison of the experimental 2p excitation with some typical calculations is performed in figure 9. For the sake of clarity only the averaged curves through the experimental data are included. The universal curve, derived by Janev and Presnyakov (1980), shows a qualitative agreement with the experimental data, in particular if one considers the strong simplifications in its derivation. Their influence on the result was studied by Fritsch and Schartner (1987), though the three-state approximation was still used. In this calculation no scaling of the cross sections was observed. Substitution of the three-state base by a considerably extended base resulted once more in a scaling of the cross sections for scaled energies higher than 15 keV u^{-1} and for projectile charges $q \geqslant 2$. The predicted scaled excitation function shows an excellent agreement with our data. The only difference between theory and experiment lies in the fact that the experimental data scale for $q \geqslant 3$ while the calculated cross sections for $q \geqslant 2$.

A significant simpler theoretical approach to the problem offers distorted wave calculations in the eikonal impulse approximation of Rodriguez and Miraglia (1992). Also in their model the scaled cross sections converge against an universal curve with increasing projectile charge, but the experimental data are underestimated by about 20%. Furthermore the shift of the cross section maximum with q toward lower energies is not described.

A different way to study the q dependence of excitation cross sections is to keep the impact velocity constant and to increase q. This is done for an energy of 286 keV u^{-1} in figure 10. The 2p excitation cross section shows a saturation tendency, especially when compared with the q^2 proportionality of the FBA, included in figure 10. For the first time Brendlé *et al* (1985) measured such a behaviour for the 1s–2p excitation of

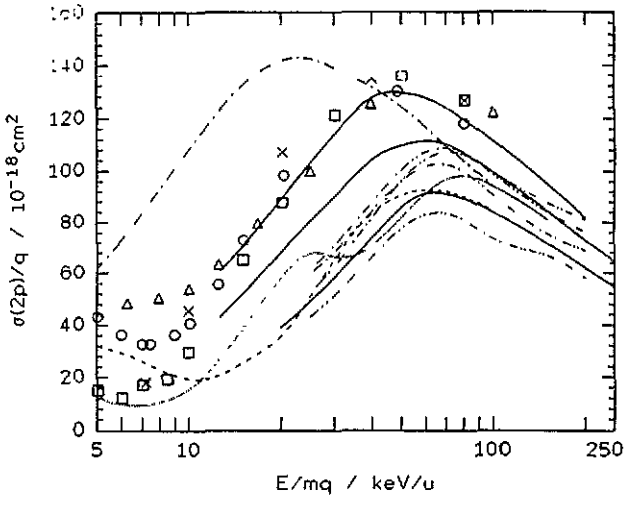

Figure 9. Scaled cross sections for the excitation of the 2p state by Cu and Si ions, comparison with theory. Curves for the experiments and for each theory are drawn with the same linestyle. The larger the cross sections the higher the charge of the projectile. Experiment: ——, averaged data for excitation by protons, He^{2+}, Si^{q+} and Cu^{q+}. Theory: — · —, the universal curve of Janev and Presnyakov (1980); ○, $q=2$; □, $q=4$; △, $q=8$; ×, $q=16$, AO+, Fritsch and Schartner (1987); - - -, excitation by protons, AO+ Fritsch and Lin (1983); — · · —, EIA⁻, for $q=1$, 2, 4 and 8, Rodriguez and Miraglia (1992); · · · ·, He^{2+}, AO+, Fritsch *et al* (1991).

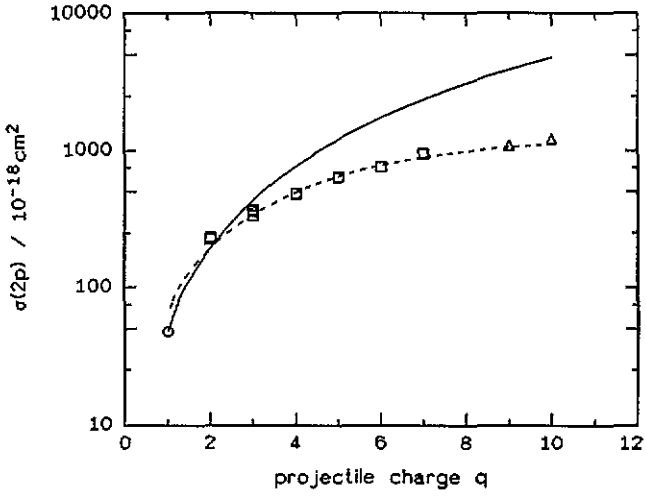

Figure 10. Cross sections for the excitation of the 2p state by Cu and Si ions with energy of 286 keV u^{-1} for various projectile charges q. Experiment: ○, protons; □, Si^{q+}; △, Cu^{q+}; Theory: ——, cross sections according to the FBA scaled by q^2; - - -, cross sections derived from the universal experimental curve for $q \geq 3$ by the JP scaling.

Fe^{24+} at a velocity of 17 au and introduced the term 'saturation'. They performed variational calculations and explained the 'saturation' by the appearance of second-order terms. Reymann *et al* (1988) confirmed this behaviour for the excitation of He atoms and very recent measurements of Chabot *et al* (1994) showed the same effect for

the 1s–2p excitation of Kr^{34+} at velocities of 35 au. Furthermore Datz *et al* (1990) observed a 'saturation' behaviour of the ionization of He by highly charged ions.

However in all mentioned experiments this slow increase of σ and q is not a matter of saturation but just a consequence of the validity of the JP scaling. Due to this relation the cross section increases linearly with the charge q and the maximum of the cross section is shifted toward higher energies as q increases. Assuming the validity of the FBA for the excitation of the H(2p) level by protons for energies higher than 200 keV, one should not expect the validity of the FBA for excitation by projectiles with higher q values at energies below $q \times 200$ keV u^{-1}. This becomes very clear from figure 11 where the unscaled cross sections for the excitation of the H(2p) level by projectiles with various charges q are displayed. The curves are calculated from the scaled universal experimental curve for $q \geqslant 3$ using the JP scaling. Cross sections at the cut at 286 keV u^{-1} are included in figure 10, and are in very good agreement with the experimental data. In conclusion, experiments that test saturation of the cross section should be performed at sufficiently high energies, where the FBA should be valid for the projectiles with the highest investigated charge q.

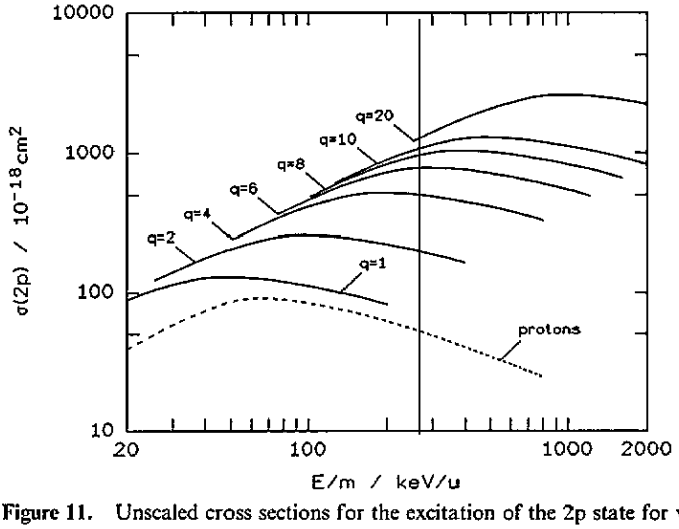

Figure 11. Unscaled cross sections for the excitation of the 2p state for various projectile charges q. The curves have been calculated from the universal experimental curve for $q \geqslant 3$ by the JP scaling. For comparison proton data are included.

3.4. Results for the higher np states ($n \geqslant 3$)

Figure 12 shows the cross sections for the H(np) levels with $n \geqslant 3$ for proton impact scaled by the relation:

$$\sigma(n\mathrm{p})_{\mathrm{scaled}} = \sigma(n\mathrm{p}) \times (\sigma(2\mathrm{p})/\sigma(n\mathrm{p}))_{800\,\mathrm{keV}}/\sigma(2\mathrm{p})_{\mathrm{max}} \qquad (4)$$

where $\sigma(2\mathrm{p})_{\mathrm{max}}$ denotes the maximum of the 2p cross section. All cross sections have in the energy range of our experiments the same energy dependence. Because they are normalized to the FBA at high energies, they also scale, with respect to the main quantum number n, at low energies like the FBA.

Since the cross sections of the np states with $n \geqslant 3$ show the same energy dependence as the cross section of the 2p state, the mean curve of the 2p state can be scaled with the factors given in table 1 to obtain averaged cross sections for the other states. These

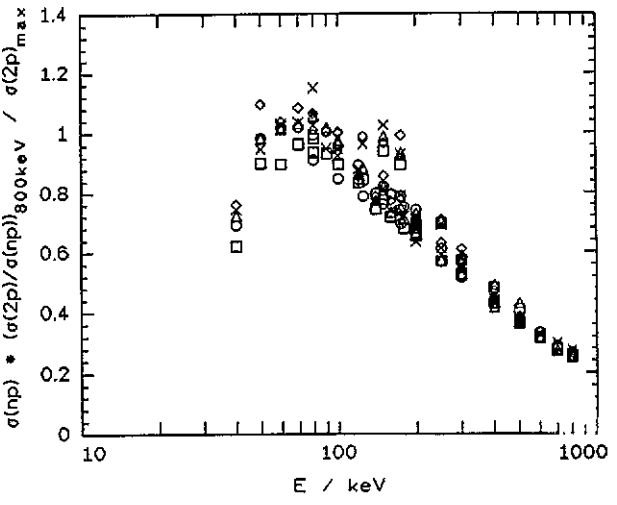

Figure 12. Cross sections for the excitation of the *n*p states by protons, each scaled according to ordinate. ○, 2p; □, 3p; △, 4p; ◇, 5p, ×, 6p.

Table 1. Ratios of the cross sections for excitation of the *n*p states and the 2p state cross section after excitation by protons.

$\sigma(2p)/\sigma(np)$				
2p	3p	4p	5p	6p
1	5.93	16.5	34.1	62.7

curves are needed for comparison with the data for highly charged ion impact (figures 13 and 14). The averaged values of the *n*p states ($n \geqslant 3$) for energies less than 40 keV are not supported by data points and thus are only an estimation. They depend on the assumption that the *n*p-state cross sections have the same energy dependence below 40 keV as the cross sections of the 2p state. This assumption is confirmed by measurements with He^+ projectiles, which are displayed unscaled together with the cross sections for the excitation by He^{2+} ions in figure 13. The *n*p cross sections show the same energy dependence as the cross sections for the 2p state and scale with the same factors as in the H^+–H system of table 1. A somewhat different situation appears in the Si^{q+} and Cu^{q+}–H systems, displayed in figure 14. All cross sections show the same energy dependence, but the scaling is slightly different from the H^+–H system. Here the scaled cross sections for the excitation of the *n*p states ($n \geqslant 3$) can be derived from the scaled cross section of the He^{2+}–H system, thus the JP scaling holds for projectile charges $q \geqslant 2$.

3.5. Cross sections for H(2p) excitation in He^+, Ne^+–H collisions

Finally, experiments with single charged He^+ and Ne^+ ions are described and discussed in comparison with the data of the previous sections. He^+ and Ne^+ ions with energies between 15 keV u^{-1} and 200 keV u^{-1} and 4 keV u^{-1} and 40 keV u^{-1}, respectively, were available. The cross sections for excitation of the 2p state by He^+ and Ne^+ ions are shown in figure 15. For comparison the data of McKee *et al* (1977), who measured the 2p excitation by He^+ ions, and the cross sections for excitation by protons of Kondow

Table 2. Cross sections in 10^{-18} cm^2 for the excitation of the H(np) states by protons, normalized to the FBA for excitation by protons at energies between 500 and 800 keV.

E (keV)	2p	3p	4p	5p	6p
40	62.9	9.50	3.91	1.95	1.06
50	89.4	13.8	5.32	2.80	1.34
60	92.5	13.7	5.49	2.65	1.46
70	92.7	14.7	5.59	2.77	1.47
80	86.6	11.5	5.73	2.70	1.54
90	91.4	14.3	5.51	2.57	1.35
100	82.1	13.7	5.26	2.56	1.33
120	81.2	12.8	4.68	2.15	1.25
125	71.7	12.9	4.79	2.53	1.37
140	72.6	11.4	4.19	2.01	1.08
150	72.0	13.2	4.90	2.33	1.30
160	72.3	11.0	3.97	1.97	1.05
175	67.4	12.5	4.56	2.27	1.22
180	68.3	10.4	3.86	1.79	1.02
200	63.6	10.3	3.79	1.82	0.952
250	53.6	9.65	3.46	1.71	0.923
300	47.1	8.39	3.01	1.51	0.784
400	39.5	6.94	2.45	1.20	0.617
500	34.3	5.91	2.14	0.959	0.538
600	30.5	4.84	1.70	0.853	0.466
700	26.1	4.20	1.46	0.721	0.423
800	24.2	3.88	1.35	0.647	0.389
Errors	12%	13%	14%	16%	18%

Table 3. Cross sections in 10^{-18} cm^2 for the excitation of the H(np) states by He^+ ions, normalized to the FBA for excitation by protons at an energy of 300 keV.

E (keV)	2p	3p	4p	5p	6p
60	51.7	9.04	3.40	1.58	0.740
80	66.8	11.4	4.57	1.97	0.940
100	77.1	12.9	5.18	2.44	1.14
125	82.8	14.4	5.71	2.60	1.31
150	90.8	15.5	6.16	2.78	1.51
175	92.7	16.1	6.41	3.05	1.49
200	91.7	16.2	6.22	3.01	1.49
250	93.0	16.4	6.40	3.00	1.45
300	90.0	16.1	6.03	2.91	1.49
400	90.1	15.9	5.92	2.86	1.44
500	83.1	14.1	5.41	2.55	1.21
600	78.2	13.3	4.89	2.49	1.26
700	73.2	12.6	4.58	2.20	1.11
800	67.6	11.9	4.16	2.23	1.18
Errors	17%	13%	14%	17%	20%

et al (1974) and our group are included. To our knowledge no theoretical data for the Ne^+–H system exist and only a few calculations handle the excitation into the H(2p) state by He^+ ions, so we disregarded any calculations in figure 15 and our intention is to compare the different behaviour of the cross sections after collisional excitation by H^+, He^+ and Ne^+ ions.

Table 4. Scaled cross sections in 10^{-18} cm^2 for the excitation of the H(np) states by $^3He^{2+}$ ions, normalized to cross sections for excitation by He^+ at 60, 80 and 110 keV.

E (keV)	2p	3p	4p	5p	6p
240	104.3	17.7	6.93	3.49	2.13
300	110.2	19.5	7.33	3.67	2.07
360	112.7	19.2	6.90	3.71	2.03
420	112.3	19.7	7.13	3.19	1.74
480	102.8	17.5	6.40	3.01	1.64
560	106.7	19.1	6.61	3.29	1.90
600	106.9	18.0	6.38	3.04	1.64
660	97.0	16.9	6.11	2.60	1.58
720	94.0	15.8	5.51	2.64	1.34
Errors	27%	24%	26%	32%	38%

Table 5. Cross sections in 10^{-18} cm^2 for the excitation of the H(np) states by Ne^+ ions, normalized to cross sections for excitation by He^+ at 100, 200 and 400 keV and protons at 400 keV.

E (keV)	2p	3p	4p	5p	6p
80	70.7	5.13	2.25	0.810	0.433
100	62.1	5.88	2.30	1.17	0.624
125	59.3	7.00	2.28	1.22	0.546
150	47.8	7.04	2.32	1.01	0.518
175	44.3	7.23	2.50	1.07	0.547
200	39.7	7.12	2.51	1.04	0.536
250	35.2	6.45	2.52	1.04	0.566
275	31.4	5.81	2.39	0.990	0.503
300	33.6	6.21	2.58	1.13	0.525
350	32.1	5.63	2.44	1.00	0.523
400	39.8	7.07	3.23	1.32	0.769
500	39.7	6.93	3.23	1.35	0.684
600	42.9	7.38	3.66	1.44	0.823
700	46.8	7.99	4.18	1.61	0.845
800	49.4	8.39	4.41	1.50	0.758
Errors	18%	14%	20%	18%	21%

The cross sections after excitation by He^+ ions show an energy dependence very similar to the cross sections for excitation by H^+ ions. The data suggest a minimum in the cross section at $\sim$10 keV u^{-1}, where it also appears in the H^+–H system. The height of the maximum is equal for excitation by He^+ and H^+ ions and appears approximately at the same energy. At energies higher than 100 keV u^{-1} the cross sections decrease in the same manner as the cross sections for the excitation by protons. On the low energy side of the cross section maximum the helium data do not decrease as fast as the proton data towards smaller energies.

A different shape of the cross section is observable in the Ne^+–H system. In this system also a minimum at an energy of about 12 keV u^{-1} is observable, but towards lower energies the cross sections increase much stronger than in the case of the two other collision systems. In contrast to this situation, the rise on the high energy side of the minimum is much weaker.

Table 6. Scaled cross sections in 10^{-18} cm^2 for the excitation of the H(np) states by Si^{q+} ions, normalized to cross sections for excitation by protons at 150 and 200 keV and electrons at 3 keV.

Energy E (keV)	Projectile charge q	2p	3p	4p	5p	6p
2 800	2	129.9	18.4	7.49	3.34	2.01
4 480	2	108.3	16.3	6.96	3.49	1.71
6 000	2	99.5	16.1	6.47	3.36	1.49
8 000	2	114.5	14.6	6.42	3.40	1.65
2 000	3	107.0	12.0	5.48	2.73	1.50
4 000	3	118.6	17.2	6.64	3.26	1.58
4 200	3	127.9	18.4	6.99	3.10	1.63
5 000	3	127.7	17.5	6.32	3.08	1.73
6 000	3	129.8	17.5	6.85	3.29	1.50
6 720	3	110.3	16.2	5.92	3.06	1.30
7 000	3	116.0	16.6	5.86	2.88	1.62
8 000	3	116.5	17.0	6.22	2.99	1.55
9 000	3	101.9	15.9	5.87	2.85	1.47
10 000	3	115.0	17.0	6.36	3.14	1.31
11 000	3	100.9	14.2	5.26	2.85	1.32
12 000	3	93.0	13.5	4.71	2.02	1.08
13 000	3	98.0	15.1	5.17	2.44	1.15
14 000	3	80.4	13.2	4.77	2.42	1.25
16 000	3	87,1	12.0	4.38	2.08	1.17
5 600	4	123.2	17.6	6.48		1.71
8 000	4	120.8	16.9	6.66		1.87
8 960	4	137.5	18.8	6.80	3.14	2.03
12 500	4	105.2	15.7	5.74	2.80	1.21
7 000	5	129.7	17.2	6.85		1.51
8 000	5	127.0	18.4	7.16		1.62
11 200	5	126.6	16.3	6.05	2.99	1.77
4 000	6	137.9	14.5			
6 000	6	129.4	17.1			
8 000	6	126.4	17.9			
8 400	6	130.4	18.1	7.32	3.39	1.88
12 000	6	128.0	17.7	6.67	3.20	1.91
13 400	6	104.3	16.1	6.55	2.82	1.73
16 000	6	119.9	16.8	6.37	2.94	1.94
20 000	6	103.7	14.7	5.56	2.69	1.56
8 000	7	136.2	17.1	7.68	3.77	1.81
9 800	7	132.0	18.5	7.25	3.27	1.67
15 700	7	120.2	18.1	7.25	3.67	1.55
20 000	7	92.3	14.0	5.74	2.90	1.33
11 200	8	144.1	19.0	7.04	3.23	1.51
17 900	8	119.0	19.0	6.89	3.17	1.53
20 000	8	103.5	17.9	6.55	3.05	1.73
20 000	9	107.1	16.1	5.98	2.71	1.17
Errors		29%	25%	28%	31%	42%

Besides its intrinsic meaning the behaviour of the He^+ and Ne^+ ions in exciting H to the 2p state is of concern for the discussion of a scaling on the low energy side of the cross section maximum. Figure 15 shows for both projectiles a cross section minimum around 10 keV u^{-1}. But there is no quantitive agreement. This underlies that, for

Table 7. Scaled cross sections in 10^{-18} cm^2 for the excitation of the H(np) states by Cu^{q+} ions, normalized to cross sections for excitation by protons at 150 and 200 keV and electrons at 3 keV.

Energy E (keV)	Projectile charge q	2p	3p	4p	5p	6p
5 670	3	118.9	18.3	6.33	2.75	1.37
7 560	4	110.6	17.8	6.05	2.75	1.57
4 000	5	66.9	9.37	2.97		
5 000	5	81.8	9.80	2.92		
8 000	5	95.8	15.0	4.72	2.31	1.22
9 450	5	108.5	15.6	5.82	2.63	1.83
12 000	5	117.5	17.3	6.97	2.89	1.93
16 000	5	130.3	18.2	7.09	3.46	1.75
8 000	6	85.7	15.7	5.56		
11 340	6	107.3	15.6	5.93		
12 000	6	106.9	17.1	6.11	3.40	
24 000	6	133.7	19.1	5.34	2.73	
13 230	7	106.0	15.7	6.11	2.41	1.53
15 120	8	111.8	15.2	6.00	2.96	1.72
17 010	9	121.3	15.6	6.66	2.58	1.23
18 900	10	119.9	17.8	6.40	3.00	1.30
20 000	11	113.3	16.0	6.04	2.35	1.24
Errors		20%	16%	19%	22%	33%

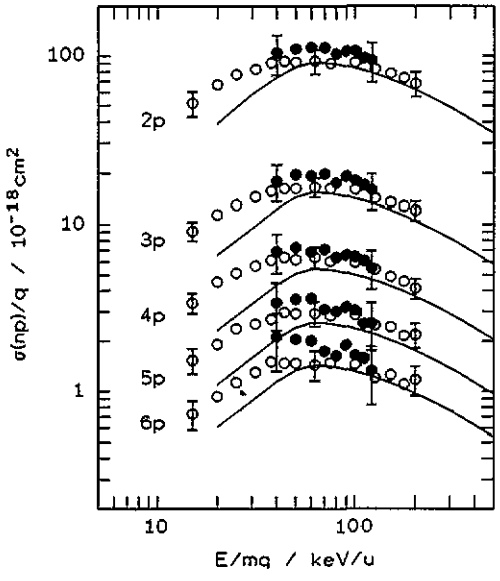

Figure 13. Cross sections for the excitation of the np states by He ions. ○, He$^+$; ●, He^{2+}; ——, experimental proton data.

a scaling in this part of the universal curve only high q values provide sufficiently large impact parameters—dominating the total cross section—which are the physical basis of the JP scaling. This condition seems to be fulfilled for the Cu ions of our experiment with $q=5$, 6 (figures 8 and 14). Whether in the here discussed scaled energy range

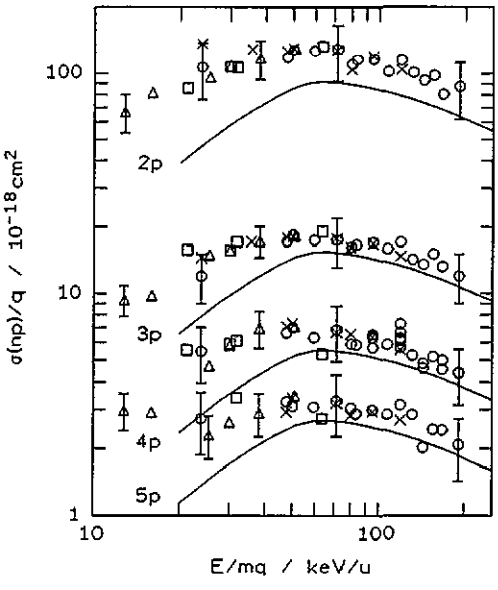

Figure 14. Scaled cross sections for the excitation of the np states by Cu and Si ions. ○, Si^{3+}; ×, Si^{6+}; △, Cu^{5+}; □, Cu^{6+}; ——, experimental proton data.

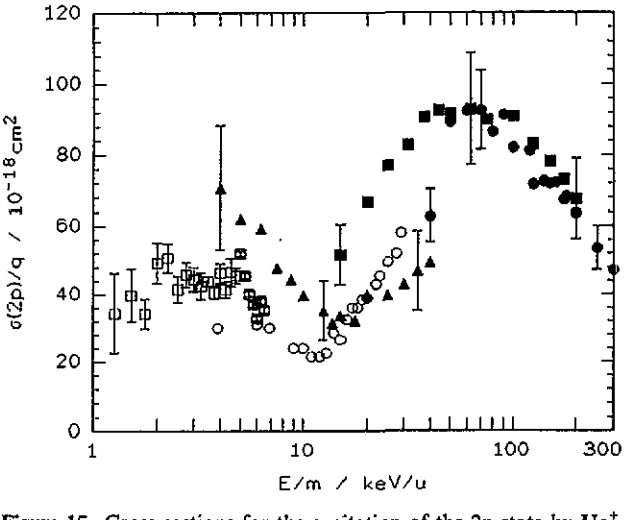

Figure 15. Cross sections for the excitation of the 2p state by He^+ and Ne^+ ions. Experiment: ●, present proton data; ○, proton data of Kondow *et al* (1974); ■, present He^+ data; □, He^+ data of McKee *et al* (1977); ▲, present Ne^+ data.

He^{2+} ions produce excitation cross sections without structures, should in our opinion be experimentally investigated further.

4. Summary and conclusions

The JP scaling relation $\sigma/q=f(v^2/q)$ has been tested for the excitation of H into the np states ($n=2,\ldots,6$) by numerous different projectiles with charges q ranging from

1+ to 11+ and with scaled velocities $v/\sqrt{q}$ ranging from less than 1 au to 6 au. The scaling relation holds for the 2p state for $q \geqslant 3$, for higher n-values for $q \geqslant 2$. The scaled universal curve lies about 40% above the curve of the H^+–H system and shows in the investigated scaled velocity range the same energy dependence. A saturation of the cross section at constant impact velocity with increasing charge could be explained as a consequence of the JP scaling. For the H^+–H system, a satisfactory data basis exists for excitation of the 2p state, but severe discrepancies exist for the cross sections of the Balmer-α line emission. The presented data for the He^{2+}–H systems underline a current interest in this system, which seems to be more sensitive to the details of close coupling calculations. The two data sets which now exist need to be completed by an independent measurement in the range of scaled energies around 40 keV u^{-1}. At this energy, the ranges of the two experiments are matching, but the data differ remarkably. This might indicate a strong structure, but might also indicate an experimental discrepancy.

The investigation of the excitation by the single charged H^+, He^+ and Ne^+ ions shows a similar energy dependence for the H^+–H and the He^+–H systems, but a different behaviour for the Ne^+–H system, which until now has not theoretically investigated.

Acknowledgments

The stimulating interest of Professor Dr Scharmann in our research and the help of Professor Heckmann and Professor Träbert and the members of their group is gratefully acknowledged. We thank the technical staff at the Dynamitron-Tandem Laboratory as well as G Trylat for their assistance. This work was supported by the Deutsche Forschungsgemeinschaft.

References

Anton M, Detleffsen D and Schartner K-H 1992 *Nucl. Fusion Suppl.* **3** 51
Anton M, Detleffsen D, Schartner K-H and Werner A 1993 *J. Phys. B: At. Mol. Opt. Phys* **26** 1
Bransden B H, Noble C J and Chandler J 1983 *J. Phys. B: At. Mol. Phys.* **16** 4191
Brendlé B, Gayet R, Rozet J P and Wohrer K 1985 *Phys. Rev. Lett.* **54** 2007
Chabot M, Wohrer K, Chetioui A, Rozet J P, Touati A, Vernhet D, Politis M F, Stephan C, Grandin J P, Martin F, Riera A, Sanz J L and Gayet R 1994 *J. Phys. B: At. Mol. Opt. Phys.* **27** 111
Clout P N and Heddle D W O 1969 *J. Opt. Soc. Am.* **59** 715
Datz S, Hippler R, Andersen L H, Dittner P F, Knudsen H, Krause H F, Miller P D, Pepmiller P L, Rosseel T, Schuch R, Stolterfoht N, Yamazaki Y and Vane C R 1990 *Phys. Rev.* A **41** 3559
Donnelly A, Geddes J and Gilbody H B 1991 *J. Phys. B: At. Mol. Opt. Phys.* **24** 165
Ermolaev A M 1991 *J. Phys. B: At. Mol. Opt. Phys.* **24** L495
Fritsch W and Lin C D 1983 *Phys. Rev.* A **26** 762
—— 1991 *Phys. Rep.* **202** 1
Fritsch W and Schartner K-H 1987 *Phys. Lett.* **126**A 17
Fritsch W, Shingal R and Lin C-D 1991 *Phys. Rev.* A **44** 5686
Henne A, Luedde H J, Toepfer A, Gluth T and Dreizler R M 1993 *J. Phys. B: At. Mol. Opt. Phys.* **26** 3815
Hughes M P, Geddes J and Gilbody H B 1993 *Proc. 18th Int. Conf. on the Physics of Electronic and Atomic Collisions* (*Aarhus*) ed T Andersen, B Fastrup, F Folkmann and H Knudsen (Aarhus: University of Aarhus) Abstracts p 491
Janev R K, Boley C D and Post D E 1989 *Nucl. Fusion* **29** 2125
Janev R K and Presnyakov L P 1980 *J. Phys. B: At. Mol. Phys.* **13** 4233
Kondow T, Girnius R J, Chong Y P and Fite W L 1974 *Phys. Rev.* A **10** 1167
Mandal C R, Mandal Mita and Mukherjee S C 1990 *Phys. Rev.* A **42** 1787
Massey H S and Gilbody H B 1974 *Electronic and Ionic Impact Phenomena* (Oxford: Clarendon)

McKee J D A, Sheridan J R, Geddes J and Gilbody H B 1977 *J. Phys. B: At. Mol. Phys.* **10** 1679
Morgan T J, Geddes J and Gilbody H B 1973 *J. Phys. B: At. Mol. Phys.* **6** 2118
Park J T, Aldag J E, George M and Peacher J L 1976 *Phys. Rev.* A **14** 608
Reinhold C O, Olson R E and Fritsch W 1990 *Phys. Rev.* A **41** 4837
Reymann K, Schartner K-H, Sommer B and Traebert E 1988 *Phys. Rev.* A **38** 2290
Rodriguez V D and Miraglia J E 1992 *J. Phys. B: At. Mol. Opt. Phys.* **25** 2037
Shakeshaft R 1978 *Phys. Rev.* A **18** 1930
Slim H A 1993 *J. Phys. B: At. Mol. Opt. Phys.* **26** L743
—— 1994 *J. Phys. B: At. Mol. Opt Phys.* **27** L203
Stebbings R F, Young R A, Oxley C L and Ehrhardt H 1965 *Phys. Rev.* A **138** A1312